Soft Matter

Cite this: *Soft Matter*, 2012, **8**, 1977

www.rsc.org/softmatter

PAPER

Electrophoretic stretching of tethered polymer chains by travelling-wave electric fields: tunable stretching, expedited coil–stretch transition, and a new paradigm of dynamic molecular probing

Yen-Ching Li, Ten-Chin Wen and Hsien-Hung Wei*

Received 2nd August 2011, Accepted 8th November 2011
DOI: 10.1039/c1sm06485a

The use of low-frequency travelling wave fields in electrophoretic stretching of charged polymer chains is investigated theoretically. We find, using a simple elastic dumbbell model, that the stretching behavior with and without fluctuations can show a number of distinctive features that cannot be seen in usual steady or alternating current electric fields. In the deterministic study without fluctuations, we show that an end-tethered charged polymer chain can be pulled by asymmetric strokes generated by a travelling wave field and kept extended along the wave. It is found that while the averaged chain extension can be increased by raising the field strength, it can be decreased by increasing the wave speed. This is a new example that stretching a polymer chain can be realized in a time periodic field with zero mean. As the free energy landscape here acts like a vibrating harmonic oscillator having double or multiple wells, a stretched chain trapped in an energy groove created by a travelling wave field can hop back to the lower energy coil state due to fluctuations. In this stochastic study, we develop a theory and carry out Brownian dynamics simulations to show that as long as the wave speed does not exceed the damping threshold and fluctuations do not prevail to diminish stretching, increasing the wave speed can help the chain maintain its stretch by preventing it from hopping to the coil state. In addition, two distinct hopping kinetics, Arrhenius and Kramers modes, can exist to govern the respective coil–stretch transitions in the double-well and multiple-well scenarios, depending on the extent of stretching. These features are the results of cooperative effects of travelling wave fields and fluctuations, and further manifested by tongue-like coil–stretch phase diagrams. Applications of the present stretching to dynamic molecular probing are also illustrated by monitoring and regulating the molecular transport over a cyclically stretching polymer chain at the nanoscale or single-molecule level.

I. Introduction

Stretching of a single polymer chain not only provides an understanding of how it responds mechanically to external forcing, but also spurs new research and technological developments. Many of these developments involve manipulation of DNA, through utilizing its basepair matching and ability to bind other molecules along its backbone, for realizing molecular probing and detection at the single molecule level. For instance, one can stretch out an entire DNA molecule to perform more direct reading and mapping of the encoded genetic information along the chain.[1,2] By analyzing the stretching response of DNA, its interactions with protein or other ligand molecules can be detected and quantified in an ultrasensitive manner.[3] This single molecule force spectroscopy technique has been further exploited to monitor the replication of a single DNA polymerase along single stranded DNA.[4]

Department of Chemical Engineering, National Cheng Kung University, Tainan, 701, Taiwan. E-mail: hhwei@mail.ncku.edu.tw

In addition to biological relevance, the control of folding/unfolding of a polymer chain is essential in many contexts of polymer science and technology. One of the issues is often concerning self-assembly of polymer chains. Whether chains are coiled or stretched is crucial to how they interact with neighboring molecules and hence to how their assembly is shaped. For instance, a stretched charged polymer chain, because of the ln (r) dependence on its electrostatic potential, is capable of attracting oppositely charged ions distantly, where r is the polymer-ion distance. This is the well-known counterion condensation,[5,6] which can lead to more compact self-assembled structures due to non-trivial interactions between the chain and condensed counterions.[7] In contrast, the coiled form can only arrest nearby ions due to the much rapid $1/r$ decay in its potential, resulting in much weaker electrostatic interactions. This geometry-sensitive feature in molecular interactions could be further utilized to enhance molecular sensing or to facilitate formation of ordered structures under the influence of external fields. For instance, by stretching DNA that contains target-specific probes along its backbone, it is possible to capture more target molecules for increasing the

detection efficiency. It has also been observed that DNA molecules can crumple into mesoscale bundles when they are stretched in dense surfactant brushes.[8]

There are many approaches to stretching polymer chains. Perhaps the most efficient way is to pull a polymer chain at one end while having the other fixed at a surface. One advantage of this approach is that it provides a direct way for assessing how the chain extension varies with applied stretching forces at the single molecule level, as demonstrated by using optical tweezers,[9] magnetic pulling,[10] hydrodynamic flows,[11] electric fields,[12] *etc.* Since most situations involve manipulations of polyelectrolytes such as DNA, we restrict our attention to stretching of a charged polymer chain under electric fields and seek a new strategy for controlling its stretching behavior.

In this work we propose the use of travelling wave electric fields in stretching a tethered polymer chain. Why we are interested in such stretching is motivated by our recent study on electrophoretic trapping of charged particles in travelling wave fields.[13] In that study, we found that a charged particle can exhibit a net displacement after a cycle under the influence of travelling wave fields, as opposed to the zero time-averaged movement in a purely sinusoidal field. In particular, particles could fall into one of the stable fixed points created by the field and then move alongside with it. In other words, a travelling wave field can create a moving trap array to lock and ship charged particles simultaneously. Therefore, if a charged polymer chain was placed in such a field, it would undergo similar synchronized trapping and get extended with the help of holding one end. As such stretching can be further mediated by the wave speed, this might provide an additional means for controlling the extent of stretching. Moreover, because the free energy landscape here constantly changes with time, this could affect how a chain changes from the stretched state to the coil state due to fluctuations. In other words, new impacts on coil–stretch transition[14] could emerge due to combined effects of travelling wave fields and fluctuations.

Motivated by the above, we would like to theoretically examine how an end-tethered polymer chain gets extended under the actions of travelling wave fields. Here we focus on the stretching in the low frequency regime, so that it is driven solely by electrophoresis but not by dielectrophoresis that dominates at high frequencies.[15] We also do not intend to study detailed chain conformational changes, which could involve complicated folding and unfolding dynamics. Instead, we employ a simple elastic dumbbell model to reveal how a polymer chain responds to travelling wave fields as well as to illuminate essential physics underlying the stretching. In this work, both deterministic and stochastic dynamics will also be examined respectively without and with fluctuations. In the deterministic study, we will identify the stretching mechanism and how the chain extension is determined by the strength and speed of an applied traveling field (Sections V and VI). After understanding how the stretching is determined by travelling wave fields, in the stochastic study (Section VIII) we will then explore how fluctuations play roles in the coil–stretch transition so as to see how the effects compete with those found in the deterministic study. As will be demonstrated shortly, the features of the stretching in both deterministic and stochastic studies differ significantly compared to those in steady or simple sinusoidal fields. In addition, we will also illustrate the use of traveling-wave stretching in molecular probing and detection (Section IX).

II. Modeling of chain dynamics

We first describe how to realize stretching of a polymer chain using travelling wave fields. Travelling wave signals can be generated by an array of microelectrodes subject to sequentially phase-shifted voltages on the upper surface of a microchannel (see Fig. 1). In this setup, the electrodes have equal width and separation of size ℓ much larger than the channel depth h. The resulting electric field, because of this length scale disparity, can generate nearly unidirectional strokes[13] to pull a polymer chain tethered at the bottom surface of the channel.

The chain is modeled as a simple elastic dumbbell in which two charged beads are connected by a Hookean spring with the spring constant, k. Further assume that these beads have the same electrophoretic mobility μ and drag coefficient ζ. The applied travelling wave field, for simplicity, can be taken as a simple harmonic form: $E = E_0\sin(b(x - ct))$, where x is the position in reference to the fixed end of the chain, E_0 the field strength, $b = (\pi/4)\ell^{-1}$ the wave number, and c the travelling speed of the field. In addition to the drag force $\zeta \mathrm{d}x/\mathrm{d}t$, elastic restoring force $-kx$ and electric stretching force $\zeta\mu E_0\sin(b(x - ct))$, we also include fluctuation effects by adding a random force $\xi(2\zeta k_\mathrm{B}T/\Delta t)^{1/2}$ at the free end of the chain, where $k_\mathrm{B}T$ is the thermal energy and $\xi \in (-1,1)$ the randomly distributed displacement. Balancing all these forces, we derive the equation governing the stretching as $\zeta \mathrm{d}x/\mathrm{d}t = -kx + \zeta\mu E_0\sin(b(x - ct)) + \xi(2\zeta k_\mathrm{B}T/\Delta t)^{1/2}$. Let $X = bx$ and $\tau = t/t_0$ be the dimensionless length and time rescaled respectively by the spatial periodicity b^{-1} and the associated time scale $t_0 = b^{-1}/U_0$ in terms of the electrophoretic velocity $U_0 = \mu E_0$. By writing $\varepsilon(X - \alpha\tau) \equiv \sin(X - \alpha\tau)$, the equation can be re-written in the following dimensionless form:

$$\frac{\mathrm{d}X}{\mathrm{d}\tau} = -\frac{1}{De}X + \varepsilon(X - \alpha\tau) + \beta\frac{\xi}{(\Delta\tau)^{1/2}}. \qquad (1)$$

There are three dimensionless parameters characterizing the stretching. The first one is the Deborah number $De = \zeta U_0 b/k$ that measures how strong the applied stretching force is compared to the elastic restoring force. This number can also be interpreted as

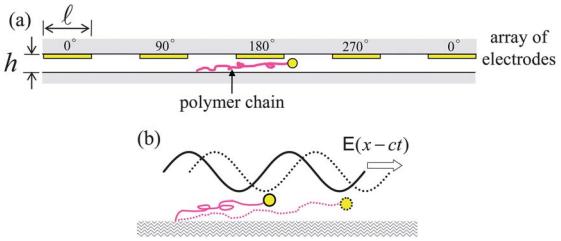

Fig. 1 (a) Schematic diagram for a device setup for stretching a tethered polymer chain in a travelling wave field. Travelling wave signals are generated by an array of microelectrodes subject to sequentially phase-shifted voltages on the upper surface of a microchannel. The electrodes have equal width and separation of size ℓ much larger than the channel depth h. The chain can be pulled by unidirectional strokes generated by a travelling field, as illustrated by schematic figure (b).

the ratio of the chain's elastic relaxation time $\tau_{relax} = \zeta/k$ to the stretching time b^{-1}/U_0. The second one is $\alpha = c/U_0$. It reflects how fast a field travels relative to the chain's electrophoretic speed. The last one is $\beta = (2k_BT/\zeta U_0 b^{-1})^{1/2}$ which measures the size of fluctuations relative to the applied field.

Several remarks are worth making concerning our model. First, this model only involves a single Hookean spring. The model better holds in the small extension regime in which chain extensions usually do not go beyond 30% of the contour length.[16,17] In fact, the applicability of this model can be better justified by inspecting stretching of long polymer chains such as DNA in the absence of fluctuations. In a typical setup, a travelling wave field of $E_0 \approx 10^2$ to 10^3 V cm^{-1} and $c \approx 10^2$ to 10^3 μm s^{-1} can be generated by applying several phase-shifted voltages of ~1 V at 1–10 Hz in an array of microelectrodes of size $\ell \approx 10$ to 100 μm. The typical mobility of DNA is $\mu \approx 10^4$ μm^2 V^{-1} s^{-1}, giving the electrophoretic velocity $U_0 = \mu E_0 \approx 10^2$ to 10^3 μm s^{-1}. Consider stretching of T4 DNA (165 kbps with contour length = 56 μm) whose coil size $R_g \approx 1$ μm and relaxation time $\tau_{relax} \approx 1$ s. These data give $De = \tau_{relax}/(\ell/U_0) \approx 1$ to 10 and $\alpha = c/U_0 \approx 1$ to 10. Because the extent of stretching is either ℓDe or $\ell De/\alpha$ (see Section VI), the DNA molecules can be extended to about 10 μm under the conditions mentioned above. This is not more than 20% of the contour length, which is within the validity of the model. Also because fluctuations tend to reduce the chain extension, the model could even better describe the stretching in more realistic situations.

Although the actual stretching behavior can be better captured by a more sophisticated model with more than one spring (for instance, using the bead-spring chain model), our single-spring model provides the following advantages. First, this simplified model allows us to obtain simple scaling relationships in terms of De, α, and β for qualifying how stretching is influenced by the field strength, the wave speed and the size of fluctuations (see Sections VI and VIII). Second, it saves a lot of computational efforts in the stochastic study for determining the fate of a polymer chain, in which both ensemble and time averages have to be evaluated (see Section VIII). In other words, it suffices to capture the essence of the stretching with minimum efforts. In addition, the results of the present study might be useful for more in-depth studies using more sophisticated models.

III. Numerical methods

We employ an ordinary differential equation solver (the Livermore solver for ordinary differential equations, LSODE)[18] to integrate eqn (1) numerically. In the absence of fluctuations ($\beta = 0$), eqn (1) is solved using the predictor-corrector Adams–Bashforth method. The chain displacement X is updated every time interval $\Delta\tau = 10^{-4}$ and within a relative error not more than 10^{-11} (the relative error here is defined as the difference of the calculated X compared to that obtained from the previous iteration using the Adams–Bashforth method). Typically, it takes about 2–50 cycles to reach a steady oscillation state, depending on De, α, and the initial value of X. After reaching a steady oscillation state, the time average value of X is taken from the data of the last cycle.

When fluctuations are present, we implement Brownian dynamics simulations according to the following procedures. Similar to the approach based on the simple Euler method, we first evaluate X, say, $X0$, by solving the deterministic part of eqn (1) using the same numerical method above within a relative error of 10^{-4}. This not only ensures consistency, but also allows us to obtain a more accurate value of $X0$ than that using the Euler method. We then add up the random force contribution $\beta\xi(\Delta\tau)^{1/2}$ for updating X according to $X(\tau + \Delta\tau) = X0(\tau + \Delta\tau) + \beta\xi(\Delta\tau)^{1/2}$. In most situations, we take $\Delta\tau = 2.5 \times 10^{-3}$ $(2\pi/\alpha)$ (equivalent to 400 time steps during a cycle) to speed up the simulations without sacrifice of the accuracy.

In each run, we take a set of different values of ξ ($\in(-1,1)$ converted from the same number of seeds generated by a random number generator with each seed standing for one value of ξ) to represent uniformly distributed random noises, and use each for calculating X every time step (*viz.*, the number of seeds is equal to that of the total time steps). For a given initial condition and a set of noises, we have also integrated eqn (1) using the Euler method and confirmed that both approaches essentially give an identical result. In addition, to ensure statistics we take different sets of random noises to repeat the simulation a number of times, say, N. This is equivalent to tracking N trajectories of X subject to different sets of random noises. In typical simulations, we take $N = 300$–1000 to ensure that the ensemble average at each time step, $\langle X\rangle$, does not change significantly with N. In terms of temporal response, it takes about 5–17 cycles for $\langle X\rangle$ to reach a steady value in the time averaged sense. The time average of $\langle X\rangle$ is taken from the ensemble-averaged data of the last two cycles. In the study on coil–stretch transition, sometimes we have to take N as high as 10 000 to assert the boundaries for the transition.

Below we begin with the deterministic study in Sections V and VI. The stochastic study will then be conducted later in Section VIII to see how fluctuations influence the stretching in competing with the effects found in the deterministic study.

IV. Asymmetric pulling and compression by travelling wave strokes

At first glance, it seems impossible to keep a polymer chain stretched in a travelling wave field because the field here is time periodic and has a zero mean. In fact, this is not the case. Similar to the motion of a charged particle in travelling wave fields,[13] a chain can exhibit an extension due to asymmetric strokes generated by a travelling wave field. Fig. 2 displays typical chain dynamics during a cycle, involving stretching, recoiling, contraction, and flipping as the chain sees different portions of a travelling wave field. When the chain sees a "hill" of the wave, it can be extended by the forward pulling if the stretching force is strong enough to oppose the elastic force (see stages I and II). As the chain further extends, the elastic restoring force could become so strong to exceed the electric pulling (*viz.*, the chain extends so fast that the field is not able to catch up with it). So the chain must retract (stage III). Right after this elastic recoil that only lasts for very short time, a "valley" of the wave emerges to reverse the field and then to compress the chain (stage IV). Adding up the pre-existing elastic force acting in the same direction, the compression will be further speeded up to cause a dramatic decrease in the chain extension. Such a compression sometimes could be so strong that the chain is flipped to against the wave (stage V). In this case, the chain could be slightly

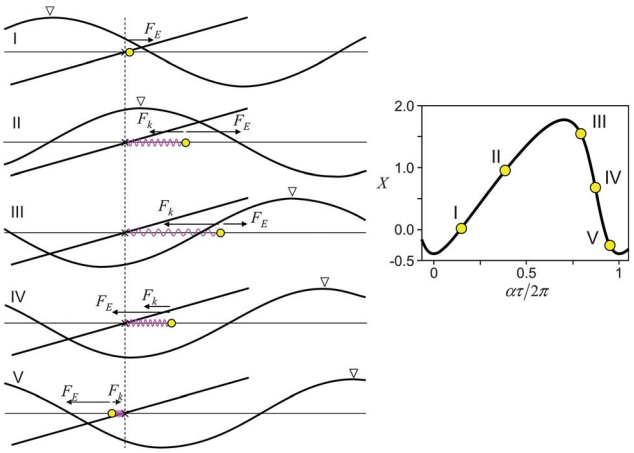

Fig. 2 Illustrated responses of a tethered polymer chain in a travelling wave field at $De = 2$ and $\alpha = 0.5$ in the absence of fluctuations. The chain can have different responses during a cycle, depending on the electric force F_E (indicated by a sinusoidal curve with a triangle mark that shows the travelling-wave movement), the elastic force F_k (indicated by a straight line), and how they exert to the chain. These responses include stretching (I & II), recoiling (III), contraction (IV), and flipping (V).

extended by the short-lived backward pulling before the succeeding wave arrives. As the next wave front strikes, the chain will soon be flipped back and then re-extended again along the wave.

As such, even though a polymer chain undergoes cyclic pulling and compression in a travelling wave field, it appears that pulling is more dominant than compression. In fact, such pulling is generated by the travelling-wave action—it is this asymmetry responsible for the observed stretch during a cycle.

V. Distinct stretching responses due to stretching–damping competition

To see how the stretching is determined by the strength and travelling speed of an applied field, we plot X against $\tau/2\pi$ for various values of De and α in Fig. 3. For $De \ll 1$, since the stretching force is insufficient to pull the chain by overcoming the elastic recoil, the chain can hardly be extended by fields regardless of α. It is clear that increasing De will promote stretching with the help of a stronger stretching force. However, the chain would lose its ability to stretch if α was too large. In this case, the chain will undergo very rapid pulling and compression. Even though the chain can be extended by forward pulling, it will soon be compressed by the reversed electric field coming from behind (see stage III in Fig. 2). Thereby, in such rapid wave strokes the chain would hardly gain an apparent extension, unless a sufficiently large De is applied to compensate for the shortage of stretching for $\alpha \gg 1$. In other words, a travelling wave field poses two opposite effects: electric pulling that tends to stretch the chain, and wave undulation that tends to damp the stretching.

It is worth pointing out that the long-term stretching behavior is independent of the sign of the chain's mobility (or charge). This is because the electric force on a polymer chain constantly changes its direction back and forth—the sign here will only introduce a phase difference and this will not change the long-term chain dynamics. So if a polymer chain can be kept stretched without flipping, its orientation will only point toward the wave propagation direction.

While $De > 1$ suffices to stretch out a polymer chain, it is not always to be able to keep the chain stretching without being flipped by periodic stroking of a travelling wave field. This implies that for a given α there must exist a critical Deborah number, De_{crit}, above which a polymer chain can always be kept extended with $X > 0$ along a wave. By plotting the dependence of

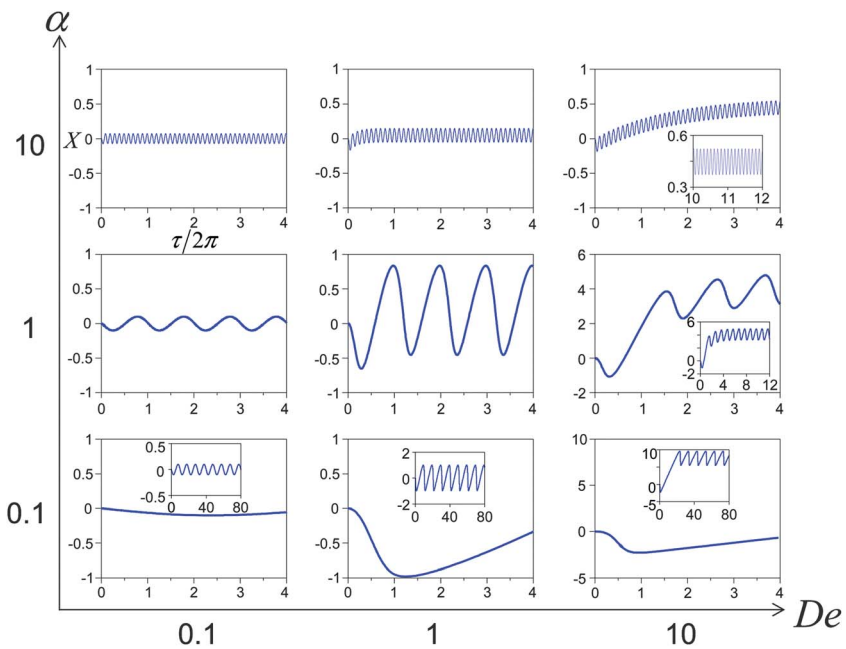

Fig. 3 Temporal evolutions of the chain displacement for various values of De and α in the absence of fluctuations ($\beta = 0$). While stretching can be enlarged by increasing De, increasing α tends to decrease stretching.

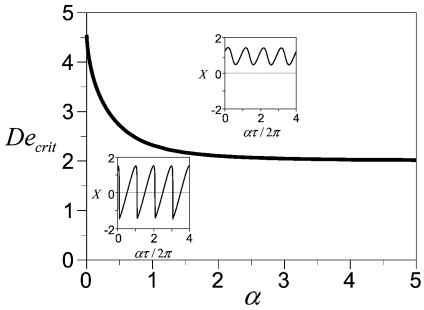

Fig. 4 The dependence of De_{crit} on α in the absence of fluctuations. Here De_{crit} is the critical Deborah number beyond which the chain can always be kept extended with $X > 0$ along the propagation direction of a travelling wave field, as illustrated in the upper inset at $De = 4$ and $\alpha = 2$. If $De < De_{crit}$, the chain can be flipped to against the field ($X < 0$) during a cycle, as seen in the lower inset at $De = 1.5$ and $\alpha = 0.01$.

De_{crit} on α in Fig. 4, we find that De_{crit} starts from 4.55 in the limit of $\alpha \to 0$, drops very rapidly for $\alpha < 1$, and reaches a constant ~2 for $\alpha > 2$. The rapid decrease of De_{crit} seen for $\alpha < 1$ implies that it is harder to maintain the stretching along a wave when the stretching is slow. This is because at small α the chain has time to be over compressed by a slowly travelling field when the field reverses its polarity. This could make the chain more susceptible to flipping and hence require a greater field to keep the chain stretched along a wave. In contrast, if the stretching is fast, the chain will not have time to be flipped by a fast moving field. So the least field required to prevent flipping will be smaller and remain unchanged as α is increased.

As the chain is constantly stretched and compressed during a cycle, we define the cycle average $\overline{(\cdot)} \equiv T_\omega^{-1} \int_{\tau'}^{\tau'+T_\omega} (\cdot) d\tau$ to measure the averaged extent of stretching, where $T_\omega = 2\pi/\alpha$ is the oscillation period. There are several choices to do this. The first obvious choice is to take the mean extension $\overline{|X|} \equiv T_\omega^{-1} \int_{\tau'}^{\tau'+T_\omega} |X| d\tau$ to measure the averaged end-to-end distance of a chain. However, it cannot tell which way the chain will orient. This question can be better answered by looking at the mean displacement $\bar{X}$ which measures the net displacement of the free end of the chain during a cycle. $\bar{X} > 0$ (<0) indicates that the chain is stretched along (against) a wave in the averaged sense. One might also be interested in the root mean square displacement $X_{rms} \equiv \sqrt{\overline{X^2}}$, as it can be used to measure the mean elastic restoring energy $\overline{X^2}/De$. All these different measures are found to be nearly identical and basically display the same feature: the averaged stretch extent is increased as De is increased, but decreased as α is increased. In fact, we find that $\bar{X}$ is always positive. Taking a cycle average for eqn (1) with $\beta = 0$, we find that the stretch is actually sustained by the averaged electric force through the balance with the averaged elastic force on the chain (because the net drag force is zero as a consequence of the reversibility of Stokes flow):

$$\frac{\overline{X}}{De} = \overline{\varepsilon(X - \alpha\tau)}. \quad (2)$$

So one can immediately recognize that $\bar{X} > 0$ is a direct consequence of $\overline{\varepsilon(X - \alpha\tau)} > 0$ resulted from the more dominant forward pulling by travelling wave fields.

It is worth pointing out that the present travelling wave stretching is very different from stretching in purely oscillatory fields. In the latter case, it can be easily shown, by setting a purely oscillatory uniform field $\varepsilon = \sin(\alpha\tau)$ in eqn (1), that $\bar{X}$ is identically zero, as the chain merely undergoes *symmetric* stretching and contraction back and forth during a cycle. This implies that spatial variations of an applied field are necessary for sustaining the stretch of a polymer chain. For a vibrating but non-traveling sinusoidal field such as $\varepsilon = \sin(X)\sin(\alpha\tau)$, we find that X will rapidly decay toward zero as time proceeds. This observation, together with that in a simple sinusoidal field, suggests that to stretch a polymer chain, if not done by a stationary field, the field not only has to be non-uniform, but also has to move for creating a ratchet-like effect.

VI. Characterization of stretching responses

In this section we would like to quantify how the stretching is determined by the strength and speed of a travelling wave field. Here we categorize the stretching into four different scenarios: weak stretching (small De), strong stretching (large De), slow stretching (small α), and fast stretching (large α), as illustrated in Fig. 5.

(i) Weak stretching ($De \ll 1$)

For $De \ll 1$, the extent of stretching is expected to be small since the electric field is too weak to pull the chain. This is because $X \approx De \ll 1$ as a result of balancing the driving travelling field term $\sin(X - \alpha\tau) \approx O(1)$ with the elastic force term X/De in eqn (1). Since the variation of the chain extension dX is also comparable to X in magnitude and the chain oscillates with time period $\tau \approx 1/\alpha$, the drag force term in eqn (1) scales as $dX/d\tau \approx \alpha De$. So this term is negligible compared to the other two $O(1)$ terms unless α is comparable or larger than $1/De$.

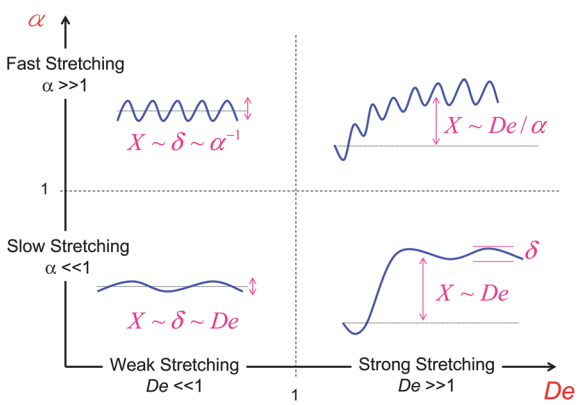

Fig. 5 Classification of stretching characteristics: weak stretching ($De \ll 1$), strong stretching ($De \gg 1$), slow stretching ($\alpha \ll 1$), and fast stretching ($\alpha \gg 1$). In each regime, how the chain displacement X and oscillation amplitude δ scale in terms of De and α is also given.

(ii) Strong stretching ($De \gg 1$)

When De is large, the chain can be readily extended by a strong field and exhibit a large extension. At a steady oscillation state, the electric force will be nearly balanced by the elastic force, giving the averaged extent of stretching: $X_{\text{steady}} \approx De \gg 1$. Because there is a small mismatch between the electric force and the elastic force at a steady oscillation state, the stretched chain will be accompanied with small variations of size $\mathrm{d}X \approx \delta \ll X_{\text{steady}}$. Thereby, the drag force term has a scale of $\mathrm{d}X/\mathrm{d}\tau \approx \alpha\delta$, which is small compared to the remaining terms in eqn (1), except for a sufficiently large α.

(iii) Slow stretching ($\alpha \ll 1$)

When α is small, the chain is stretched by a nearly stationary field. Its extension again follows $X \approx De$ because of the balance between the electric force and the elastic force. In fact, we find that the maximum chain extension in this case is precisely equal to De, as a result of the exact balance between these two forces.

(iv) Fast stretching ($\alpha \gg 1$)

For $\alpha \gg 1$, the chain is simply pulled back and forth very rapidly by a fast moving field. As the elastic force will not have time to support the stretching, the driving electric force can only be balanced by the drag generated by the rapid swaying of the chain: $\mathrm{d}X/\mathrm{d}\tau \approx \sin(X - \alpha\tau)$ with $\tau \approx 1/\alpha$, giving $\mathrm{d}X \approx \delta \approx 1/\alpha$. As the chain extension X is as small as its variation δ, the elastic force X/De scales as $1/\alpha De \ll 1$ and indeed is negligible.

To sum up, in order to get the chain extended, the electric force must be balanced by the elastic force to give $X \approx De$. When the stretching is slow, the chain will have time to develop its stretch. On the other hand, if the field strikes too fast, the elastic force will not have time to hold the extension against rapid electric strokes, thereby decreasing the extension according to $X \approx 1/\alpha$. If the stretching is both strong and fast, we expect $X \approx De/\alpha$ by combining $X \approx De$ for large De and $X \approx 1/\alpha$ for large α. Written back in the dimensional form, the actual chain extension in this particular case turns out to be $x \approx \zeta U_0^2/(kc) \propto E_0^2$—the stretch can be increased quadratically with the field strength.

The above scaling results can be seen more clearly in Fig. 6 that displays how the averaged chain extension $\overline{|X|}$ varies with De and α. Here varying α by keeping De fixed means that we vary the wave speed c independently under a fixed field strength E_0 (or U_0). On the other hand, varying De at a fixed α means that we change the electrode size b^{-1} or the chain's relaxation time $\tau_{\text{relax}} = \zeta/k$ while keeping the field strength E_0 and wave speed c fixed. Fig. 6a plots $\overline{|X|}$ against De for various values of α. For $\alpha \leq O(1)$, the extension grows like $\overline{|X|} \approx De$, regardless of the value of α. For large α (>10), the extension is small and remains nearly unchanged for small De. It starts to rise at $De \approx 1$, and then grows again according to $\overline{|X|} \approx De$ for even larger De.

Fig. 6a also reveals that at a given De, the larger the α, the smaller the $\overline{|X|}$. Such a damping becomes more evident as plotting $\overline{|X|}$ against α in Fig. 6b. At a given De, the extension remains unchanged for small α, but decays as $\overline{|X|} \approx 1/\alpha$ for large α.

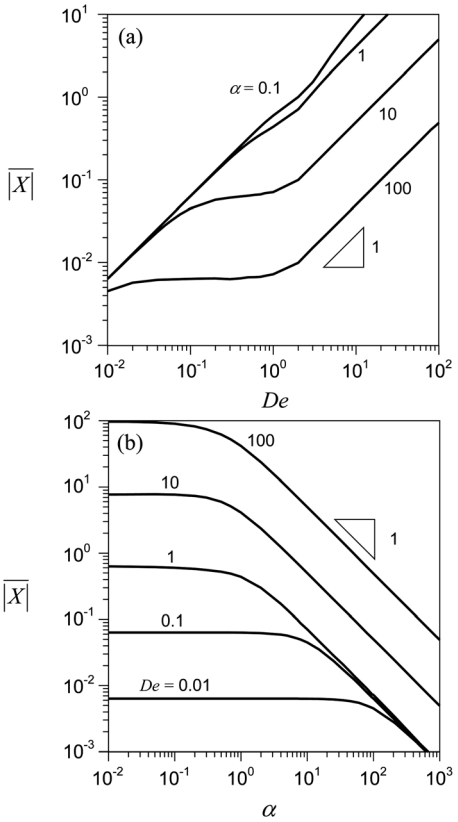

Fig. 6 Dependence of time-averaged extension on De and α in the absence of fluctuations ($\beta = 0$). (a) Plots of $\overline{|X|}$ *vs.* De for various values of α. For $\alpha \leq 0.1$, $\overline{|X|}$ virtually grows linearly with De. In this regime, the curve does not change significantly with α. For $\alpha \geq 10$, $\overline{|X|}$ remains small and nearly unchanged with De until some $O(1)$ value of De beyond which the chain regains its stretch according to $\overline{|X|} \approx De$. (b) Plots of $\overline{|X|}$ *vs.* α for various values of De. $\overline{|X|}$ with small α remains unchanged at the level of De, whereas it decays at the rate of $1/\alpha$ in the large α regime. The crossover occurs at $\alpha \approx 1/De$.

However, the transition point, α^*, between these two trends depends on the magnitude of De. For $De \leq 1$, because $X \approx De$ for small α and $X \approx 1/\alpha$ for large α, the transition occurs at $\alpha^* \approx 1/De$. On the other hand, for $De \gg 1$ we find $\alpha^* \approx 1$ as a result of the crossover between $X \approx De/\alpha$ in the large-α limit and $X \approx De$ in the small-α limit.

Based on the results of the deterministic study above, we can say that the present travelling-wave stretching is quite different from those using AC fields reported previously. Ueda and his coworkers did experimentally demonstrate the use of low-frequency sinusoidal electric fields in stretching DNA molecules in concentrated polymer solutions.[19,20] In their studies, the stretching appeared in a repetitive manner through successive hooking/releasing of DNAs with/from the surrounding polymer matrix. Recent computer simulations also revealed that polymer chains can exhibit conformational transitions in simple sinusoidal electric fields due to polarization effects.[21–23] In contrast to these studies, the present stretching is driven purely by electrophoresis *via* asymmetric pulling created by travelling wave fields. It neither involves the entanglement of a chain with the surrounding medium nor charge polarization along the chain.

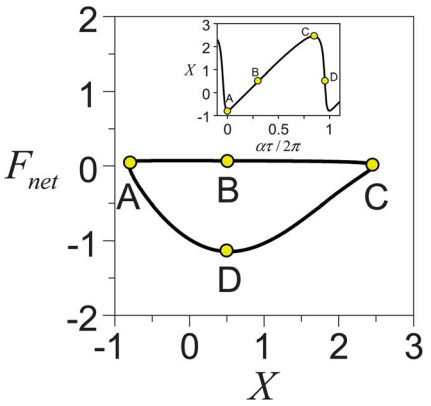

Fig. 7 Conformational hysteresis under the actions of a traveling wave field, as illustrated by plotting the net force on the chain $F_{net} = dX/d\tau$ against the chain displacement X at $De = 2.5$ and $\alpha = 0.1$. $F_{net} > 0$ (<0) corresponds to stretching (compression). Inset shows how X varies with τ. Yellow circles denote the chain's states at different times. Note that the magnitude of F_{net} during stretching is smaller than that during compression, because the electric force and the elastic force act in the same direction in the latter.

VII. Hysteresis in chain dynamics and free energy landscape

Because of asymmetric pulling and compression during a cycle, the chain would follow different paths to stretch and contract, giving rise to a hysteresis in the chain dynamics, as shown in Fig. 7. Since this irreversibility must acquire an additional work for sustaining the stretch and the work here is done by the net stretching force f_{net}, which is simply the drag force $\zeta dx/dt$ along the chain displacement, the stretching work $w_{stretch}$ can be evaluated by $\oint f_{net}dx = \int_0^{2\pi/bc}(dx/dt)^2dt$. Written in the dimensionless form, it is

$$W \equiv \frac{w_{stretch}}{\zeta U_0 b^{-1}} = \oint F_{net}dX = \int_0^{T\omega}\left(\frac{dX}{d\tau}\right)^2 d\tau. \quad (3)$$

It is clear that the stretching work is always positive, as the chain extension must change in the direction of the net force $F_{net} = dX/d\tau$—this has nothing to do with whether the chain is pulled or compressed by an electric field. Fig. 7 also reveals that the work during contraction is much greater than that during stretching. This can be understood by the fact that both electric and elastic forces during contraction act in the same direction and hence produce a much larger net force $dX/d\tau$ for compressing the chain.

An alternative view for understanding how a chain deforms in a travelling wave field can be seen by inspecting the chain's free energy landscape. The reasons for doing this are twofold. First, if fluctuations are absent as considered here, the hysteresis seen in Fig. 7 suggests that how the free energy landscape varies during stretching might behave differently compared to that during compression. It is this spatial difference in the free energies between these two opposite processes contributing to the stretching work discussed above, as will be identified shortly. Second, when fluctuations are present, because of the asymmetry between stretching and compression in the free energy, the ability to maintain the stretch would qualitatively differ from those in usual steady fields, which will be elaborated in more detail in Section VIII.

Now we derive and examine the free energy landscape as follows. Define the function $F(Z,\tau) \equiv -Z/De + \varepsilon(Z - \alpha\tau)$ to describe how the net force at a given position Z (with $Z = 0$ being the fixed end of the chain) varies with time τ. The corresponding free energy $\Phi(Z,\tau)$ can be found by integrating $F = -\partial\Phi/\partial Z$ with respect to Z. For convenience, we set $\Phi(Z = 0,\tau) = 0$ at the chain's fixed end (where Φ is the lowest when the chain is at rest). Then the free energy reads

$$\Phi \equiv \frac{\phi}{\zeta U_0 b^{-1}} = \frac{Z^2}{2De} - \int_0^Z \varepsilon(Z - \alpha\tau)dZ, \quad (4)$$

whose dimensional form ϕ has units of $\zeta U_0 b^{-1}$. Fig. 8a and b show typical spatiotemporal evolutions for Φ during a cycle when the chain undergoes apparent stretching by a strong traveling wave field. As seen in these figures, during stretching the chain's free end is situated in a moving energy downslope ($F > 0$) that is uplifted by the field (Fig. 8a), whereas it is quickly brought down by a descending upslope ($F < 0$) during contraction (Fig. 8b). In addition, how Φ changes with position and time can be better understood by considering an arbitrary differential change of Φ evaluated at the chain's free end $Z = X(\tau)$:

$$d\Phi|_X = \left.\frac{\partial\Phi}{\partial\tau}\right|_X d\tau + \left.\frac{\partial\Phi}{\partial Z}\right|_X dZ. \quad (5)$$

As can be seen more clearly in Fig. 8c, this energy change is the sum of two parts: the time varying part $\left.\frac{\partial\Phi}{\partial\tau}\right|_X d\tau = \alpha(\varepsilon(X - \alpha\tau) - \varepsilon(-\alpha\tau))d\tau$ can be recognized as the

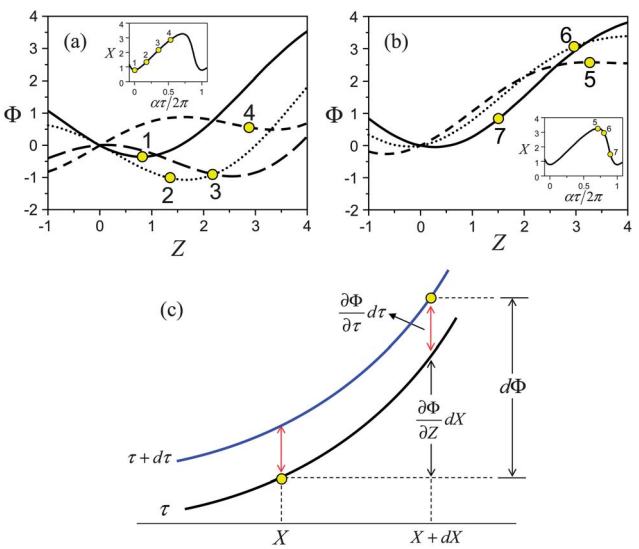

Fig. 8 Illustrated free energy landscape at $De = 4$ and $\alpha = 0.5$. Yellow circles with different numbers are used to trace how the chain's free end moves during a cycle. During stretching (a), the chain stays along an energy downslope or in a shallow well levitated by a travelling wave field, whereas it is located at an uphill rapidly moved down by the field during compression (b). (c) Schematic diagram showing how the chain's free energy change is evaluated in terms of its infinitesimal changes due to position and time.

lifting/descending work done by travelling wave strokes, and the spatial difference part comes simply from the stretching work by the chain $\left.\frac{\partial \Phi}{\partial Z}\right|_X \mathrm{d}Z = -F(X)\mathrm{d}X$.

Taking an integral over a cycle for both sides of eqn (5), and recognizing that $\oint \mathrm{d}\Phi|_X = 0$ and $\int_0^T \left.\frac{\partial \Phi}{\partial Z}\right|_X \left(\frac{\mathrm{d}X}{\mathrm{d}\tau}\right)\mathrm{d}\tau = -W$ from eqn (3), we find

$$W = \alpha \int_0^{T\omega} \varepsilon(X(\tau) - \alpha\tau)\mathrm{d}\tau. \quad (6)$$

Thereby, the stretching work, which is done by the net stretching force on the chain, is actually equal to the stroking work by a travelling wave field on the chain. As this stroking action also generates a net stretch *via* eqn (2), a direct relationship between W and averaged displacement $\bar{X}$ can then be established:

$$W = 2\pi \frac{\bar{X}}{De}. \quad (7)$$

It thus follows that the identical work is also restored into the chain through its elasticity, as it is needed for keeping the chain extended in a traveling wave field. We have also verified eqn (7) numerically, confirming the results derived in this section.

VIII. Noise-activated hopping and coil–stretch transition in a vibrating harmonic oscillator

So far we have examined the deterministic behavior of the stretching in the absence of fluctuations. When fluctuations are present, however, they can influence the dynamic stability of a polymer chain and hence modify the features seen in the deterministic study. Specifically, inevitable random thermal fluctuations could activate unraveling of a polymer coil by an external field *via* overcoming the energy barrier toward the stretched state, provided that the stretched state has a lower energy than the coil state due to the additional work done by the field on the chain (*i.e.* the last term of eqn (4)). The effects could equally reduce the extent of stretching or even make the chain shrunk back to the coiled form if the stretched state has a higher energy level with the energy barrier comparable to or less than the thermal energy k_BT. This is the well-known coil–stretch transition[14]—a kinetically trapped polymer chain can undergo hopping from one well to another by surmounting the barrier in between. This problem is actually well understood in steady fields.[24,25] In a traveling wave field, however, because the free energy landscape can vary with both position and time, whether hopping can occur would depend on if the chain has time to jump to a lower energy state before the landscape moves due to the travelling wave actions. The situation here can be thought of as a vibrating harmonic oscillator whose shape varies in such a way that De affects the depths of local energy minima and α describes how the shape oscillates with both position and time.

Prior to carrying out our analysis in detail, we should briefly discuss how the free energy profile influences the stability of a polymer chain. For $De < 1$, the free energy is dominated by the parabolic elastic well (*i.e.* the De term in eqn (4)) with a single minimum around the bottom. Since the chain extension $X \approx De < 1$ is small, the chain actually stays around the bottom of the well and is slightly swayed back and forth by it due to the relatively weak travelling-wave field. Therefore, when fluctuations are present, we expect that the chain would tend to stay like a coil. In other words, hopping is impossible unless a sufficiently strong sinusoidal field is applied to generate more than one energy minimum, which demands $De > 1$ and hence an apparent stretch.

For $De > 1$, not only do the traveling-wave undulations (*i.e.* the last term in eqn (4)) become more important to produce multiple wells in the free energy landscape, but also the chain extension is large enough to make across between these wells so that hopping from one well to another now becomes possible. A closer inspection reveals that how the shape of the free energy landscape determines hopping seems to have something to do with whether the chain can keep extended along the wave during a cycle. That is, the situation would depend if De is smaller or larger than De_{crit} (see Fig. 4). So there are two scenarios. The first is when $1 < De < De_{crit}$. While the chain in this case can show an extension in the averaged sense, it can be flipped by the field during a cycle (see the inset of Fig. 4). The corresponding free energy landscape looks like a bistable potential in which the chain sways in a seesawing manner. For $De > De_{crit}$, the chain can always keep extended without being flipped by the field. In this case, the free energy landscape can exhibit multiple wells over which the chain spans. As will be shown below, the hopping kinetics in these two scenarios can be governed by different laws.

A. Arrhenius hopping for a slightly stretched chain in double wells ($1 < De < De_{crit}$)

We first consider the case of $1 < De < De_{crit}$. In this case, a somewhat extended chain is periodically moving up and down in between two alternately rising wells on the bottom of the landscape. As displayed in Fig. 9a and b, the situation here looks as if the chains were swinging in a seesaw (but in a somewhat asymmetric manner due to the slightly dominant pulling toward the right). While the chain is trapped and stretched around the shallow well at the right, it could happen that the left well has a slightly lower energy level during a cycle, as illustrated in Fig. 9c. This allows the chain to escape from the right to the left well due to fluctuations and hence reduces the chain extension (in the ensemble averaged sense). Such a noise-activated escaping process typically occurs if the barrier height $\Delta\phi_{barrier}$ is an order of k_BT or smaller. However, since the free energy landscape constantly changes with time, the chain must jump sufficiently fast before it feels any significant change in the landscape. In terms of time scale, this demands that the hopping time $t_{hopping}$ is much shorter than the cycling period $t_{cycle} = 2\pi/(bc)$ as if hopping occurred in a stationary landscape. Conversely, one requires $t_{hopping} > t_{cycle}$ to keep the chain extended without hopping back to the left well. As the chain here is only slightly stretched around the bottom of the landscape, it must first undergo elastic recoil before escaping toward the left well in this double-well situation. In terms of probability (which is inversely proportional to the time scale of a process), the probability for the whole hopping process is the joint probability of elastic recoiling ($\propto 1/\tau_{relax}$) and escaping ($\propto \exp(-\Delta\phi_{barrier}/k_BT)$), where

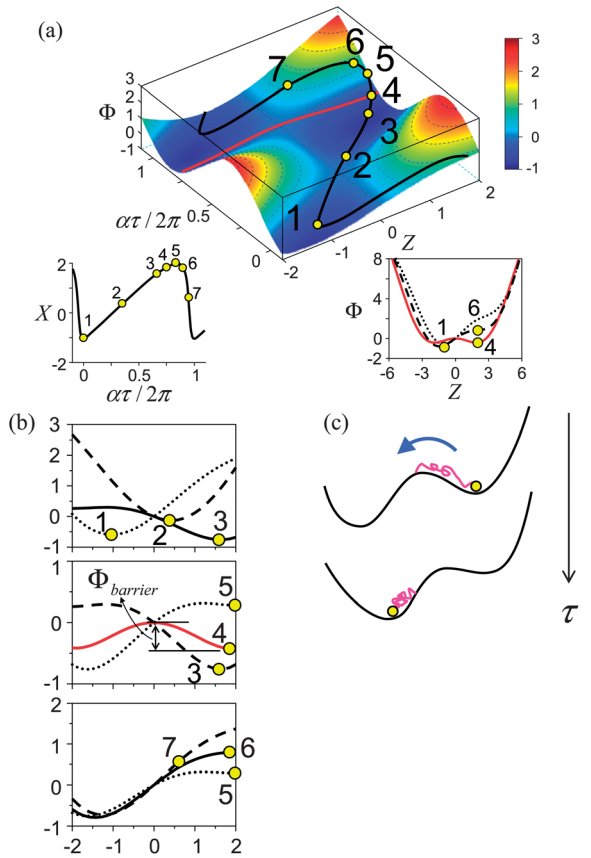

Fig. 9 Free energy landscape at $De = 2$ ($<De_{crit}$) and $\alpha = 0.1$. (a) 3d plot showing how the landscape varies with position and time. (b) Corresponding snapshots during a cycle. Yellow circles with different numbers are used to trace the sequential movement of the chain's free end during a cycle. The landscape can exhibit double wells during a cycle, as seen in (b). At stage 4 near the maximum chain extension, the chain could hop from the right well to the left well due to fluctuations if the dimensional barrier height $\Delta\phi_{barrier} = \zeta U_0 b^{-1}\Phi_{barrier}$ is comparable to or less than the thermal energy k_BT, as illustrated in (c).

$\tau_{relax} = \zeta/k$ is the chain's relaxation time. Therefore, the hopping time can be estimated by the simple Arrhenius law:

$$t_{hopping} \approx \tau_{relax} \exp\left(\frac{\Delta\phi_{barrier}}{k_BT}\right), \quad (8)$$

wherein $\Delta\phi_{barrier}/k_BT = 2\Phi_{barrier}\beta^{-2}$ with $\Phi_{barrier}$ being the corresponding dimensionless barrier height in terms of Φ by rescaling ϕ with $\zeta U_0 b^{-1}$. Since the double wells here are created by a sinusoidal field and only appear sometimes during a cycle (see Fig. 9c), the magnitude of $\Phi_{barrier}$ should never exceed the free energy associated with the field, namely, $\Phi_{barrier} \leq 1$. By treating $\Phi_{barrier} = 1$ in eqn (8) for the estimate of $t_{hopping}$, the condition $t_{hopping} > t_{cycle}$ for keeping the chain stretched is reduced to

$$\alpha > \gamma De^{-1} \exp(-2\beta^{-2}). \quad (9)$$

Here we introduce γ as a numerical pre-factor to capture the actual hopping probability $\exp(-2\ \Phi_{barrier}\beta^{-2})$ due to the occasional appearance of the double wells, as the approximated form $\exp(-2\beta^{-2})$ with $\Phi_{barrier} = 1$ is used here. So this pre-factor somewhat measures the effectiveness of hopping in such a time-varying landscape. The actual value of γ, which should be less sensitive to De, α and β, will be determined by Brownian dynamics simulations. Note that the above criterion can only be used to reflect the ability to keep the chain stretched; it does not necessarily suggest that the extent of stretching will be large.

B. Kramers hopping for a highly stretched chain in multiple wells ($De > De_{crit}$)

For $De > De_{crit}$, the chain can be greatly extended by a travelling wave field without being flipped to the other side. In this case, the undulating electric energy posed by a travelling wave field dominates to create a rippling basin of width $\sim(2De)^{1/2}$ beyond which the elastic ladder begins to emerge. Also because De is large, not only does a highly stretched polymer chain span over a number of undulating grooves, but also it is upheld by cyclically lifting and descending by a travelling wave field, as displayed in Fig. 10a and b. So the chain during stretching is actually trapped around a local minimum rising up alongside with an energy barrier toward the neighboring minimum at a lower energy level, as illustrated in Fig. 10c. In this case, the

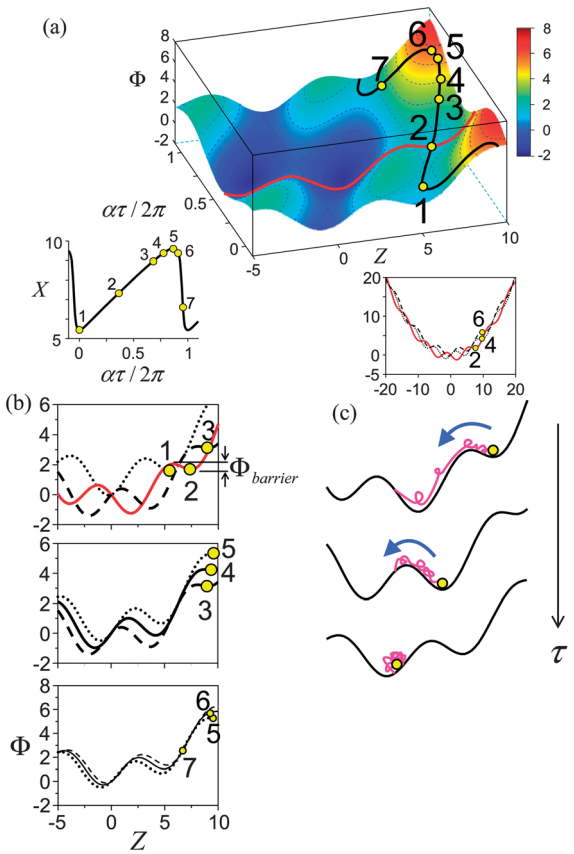

Fig. 10 Free energy landscape at $De = 10$ ($>De_{crit}$) and $\alpha = 0.1$. (a) 3d plot showing how the landscape varies with position and time. (b) Corresponding snapshots during a cycle. Yellow circles with different numbers are used to trace the sequential movement of the chain's free end during a cycle. The landscape here can possess multiple maxima and minima. In this case, the chain trapped at a higher groove could hop to a lower one due to fluctuations at any moment during a cycle, as illustrated in (c).

chain could either escape to a lower-energy stretched state or even fall all the way back to the coil state.

As the hopping here actually takes place in multiple wells created by a more dominant sinusoidal electric field, the probability for a chain jumping from one well to another would depend on the shape of the *local* free energy profile. So in this multiple-well situation, the hopping time is better described by the Kramers rate theory:[26,27]

$$t_{hopping} \approx \frac{\ell_1 \ell_2}{\mathcal{D}} \exp\left(\frac{\Delta\Phi_{\text{barrier}}}{k_B T}\right). \quad (10)$$

Here ℓ_1^{-1} and ℓ_2^{-1} are the respective radii of the curvatures of the local energy minimum and maximum around the barrier. Alternatively, ℓ_1 and ℓ_2 measure the lateral length scales over which the free energy changes by the size of k_BT around these concave and convex places. Since the grooves here vary sinusoidally in space, these length scales are of an order of the spatial periodicity b^{-1}. $\mathcal{D} = k_BT/\zeta$ is the diffusion coefficient of the chain, measuring the mobility for the chain to cross energy wells and hills. Again, by setting $\Phi_{\text{barrier}} \approx 1$, the barrier has a size of about $\Delta\phi_{\text{barrier}}/k_BT \approx 2\beta^{-2}$. Using the above estimates, the condition $t_{\text{hopping}} > t_{\text{cycle}}$ for maintaining the stretch can be re-written as

$$\alpha > \lambda\beta^2 \exp(-2\beta^{-2}), \quad (11)$$

where λ is a numerical pre-factor for capturing the actual changes in ℓ_1 and ℓ_2 in eqn (10) and its value is again determined by Brownian dynamics simulations. Note that because the left hand side of eqn (11) approaches to $\lambda\beta^2$ as $\beta \to \infty$, the associated coil–stretch boundary would be insensitive to the actual value of Φ_{barrier}, as is confirmed by our simulations.

C. Other constraints due to the wave speed and the size of fluctuations

While a stretch can be better held by increasing α according to eqn (9) or (11), a too large α would suppress stretching according to $X \approx De/\alpha$, making the chain more inclined to return to the coil state. Hence, an additional criterion for maintaining a stretch must be imposed by setting $X > 1$:

$$\alpha < \nu_1 De, \quad (12)$$

with ν_1 being an $O(1)$ numerical pre-factor. This criterion can be thought of as the damping threshold at the critical wave speed $c^* = \zeta U_0^2 b/k$ below which the apparent stretch can be realized. Therefore, eqn (12) together with eqn (9) or (11) provides a range of α within which stretching can be seen in the presence of fluctuations. If fluctuations are small ($\beta \ll 1$), the smallest α needed for maintaining the stretch, $\alpha_> = \gamma De^{-1}\exp(-2\beta^{-2})$ or $\lambda\beta^2\exp(-2\beta^{-2})$, vanishes according to eqn (9) or (11), so the chain can always be kept extended by travelling wave fields at any α below $\alpha_< = \nu_1 De$, as in the deterministic study. For $De > De_{\text{crit}}$, since $\alpha_> = \gamma De^{-1}$ from eqn (9) in the large β limit is below $\alpha_<$, stretching can be observed in the window of $\alpha_> < \alpha < \alpha_<$. For $1 < De < De_{\text{crit}}$, however, $\alpha_> = \lambda\beta^2$ from eqn (11) in the large β limit could exceed $\alpha_<$. In this case, even though stretching can be made more favorable with larger α, it has been already beyond the ability to see apparent stretching because of damping by too large α.

While the chain would tend to return to the coil state through hopping activated by noises, the extent of stretching could also be reduced due to random Brownian displacements of the free end. Thus, we expect that the apparent stretch can be seen only if $X \approx De$ is greater than the Brownian displacement $\beta(\Delta\tau)^{1/2} \approx \beta$. This yields

$$\beta < \nu_2 De, \quad (13)$$

where ν_2 is an $O(1)$ numerical pre-factor. This criterion limits the size of fluctuations below which stretching can occur. It also provides the minimum field needed for the stretching by overcoming Brownian fluctuations. In terms of the electrophoretic velocity, it occurs around $U_0^* = (k_BT\zeta^{-3}k^2b^{-1})^{1/3}$. Further making use of the chain's relaxation time $\tau_{\text{relax}} = \zeta/k \approx R_g^2/\mathcal{D}$ that links the diffusion coefficient $\mathcal{D} = k_BT/\zeta$ and the coil size R_g, we find that U_0^* is actually equal to the chain's self-diffusion velocity

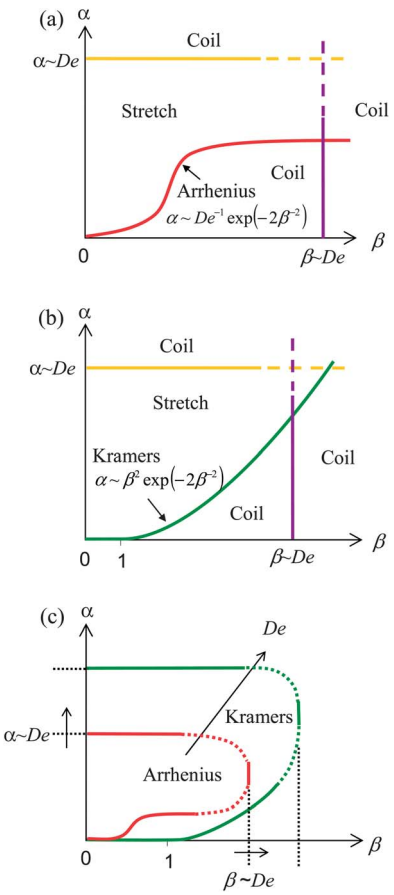

Fig. 11 Schematic illustration of coil–stretch phase diagrams under the influence of both travelling wave fields and fluctuations. The stretch region is enclosed by $\alpha \sim De$, $\beta \sim De$, and the curve determined by the hopping kinetics. For the double-well scenario with $1 < De < De_{\text{crit}}$ in (a), the hopping kinetics is of Arrhenius type, whilst Kramers-type hopping governs for the multi-well scenario with $De > De_{\text{crit}}$ in (b). (c) Combined view to illustrate how the coil–stretch phase diagram changes as De is increased. Here we use dashed lines to connect different phase boundaries to indicate smooth transitions between them.

$\mathcal{D}/R_g$ times $(bR_g)^{-1/3}$, consistent with the need in overcoming Brownian fluctuations.

D. Predicted coil–stretch phase diagram and confirmation with Brownian dynamics simulations

Fig. 11 sketches the predicted coil–stretch phase diagrams in the α–β domain according to the criteria mentioned above. For $1 < De < De_{crit}$ stretching can be seen in the region enclosed by eqn (9), (12), and (13), whilst for $De > De_{crit}$ the stretch region is bound by eqn (11)–(13). It is obvious that the stretch region in the latter is larger than that in the former, as stretching can be better maintained with larger De. It also follows that the stretch region expands as De is increased.

Now we test our theory using Brownian dynamics simulations. In our simulations, the stretched state is defined if the time average of the ensemble-averaged displacement $\overline{\langle X\rangle} > 0.5$. (Here we do not use the root mean square (rms) $\langle X^2\rangle^{1/2}$ to evaluate the extent of stretching. This is because, at a sufficiently large β, $\overline{\langle X\rangle}$ is very small but the rms value can actually turn to be very large due to large Brownian random walks.) We have confirmed (not shown) that increasing the size of fluctuation β can diminish stretching by lowering both the maximum and minimum extensions of a chain during a cycle. If fluctuations are too large, whatever the stretch it will soon be disrupted by intense Brownian fluctuations, making the chain return to the coil state (in the ensemble-averaged sense). The numerical pre-factors in eqn (9), (11)–(13) have also be determined by the simulations for capturing precise boundaries of the coil–stretch transition.

In Fig. 12, we show our simulation results for $De = 2$ and 10 corresponding to the double-well and multi-well scenarios illustrated in Fig. 9 and 10. For $De = 2$, it is found from Fig. 12a that the minimum of $\langle X\rangle$ can be increased by raising α from 0.1 to 0.5

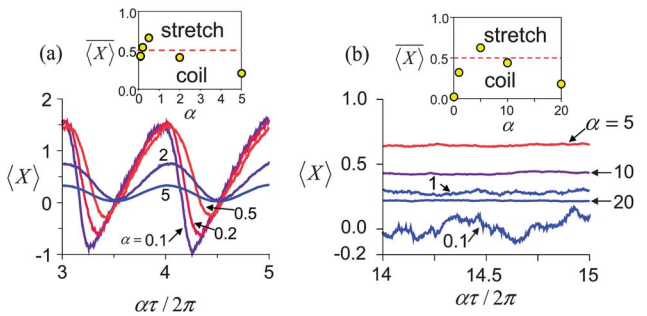

Fig. 12 Long-term temporal responses of ensemble-averaged displacement $\langle X\rangle$ at $De = 2$ and $De = 10$ in the presence of fluctuations. (a) With $De = 2$ and $\beta = 1.2$, the minimum of $\langle X\rangle$ can be increased by raising α from 0.1 to 0.5 while the maximum does not drop significantly, giving rise to an increase in the time average $\overline{\langle X\rangle}$. But further increasing $\alpha > 2$ can decrease $\langle X\rangle$ due to damping by much rapid travelling wave strokes. (b) With $De = 10$ and $\beta = 5$, the level of $\langle X\rangle$ is found to be increased by increasing α from 0.1 to 5, but decreased when increasing $\alpha > 10$. These results suggest that the stretch can be better maintained by increasing α (but not beyond the damping threshold), confirming our speculation that the decrease in the extent of stretching due to fluctuations can be prevented by diminishing the tendency of hopping *via* increasing the travelling speed. Here we use colored curves changing from red to blue for indicating the transition from the coil state to the stretched state. The insets plot the calculated $\overline{\langle X\rangle}$ as a function of α.

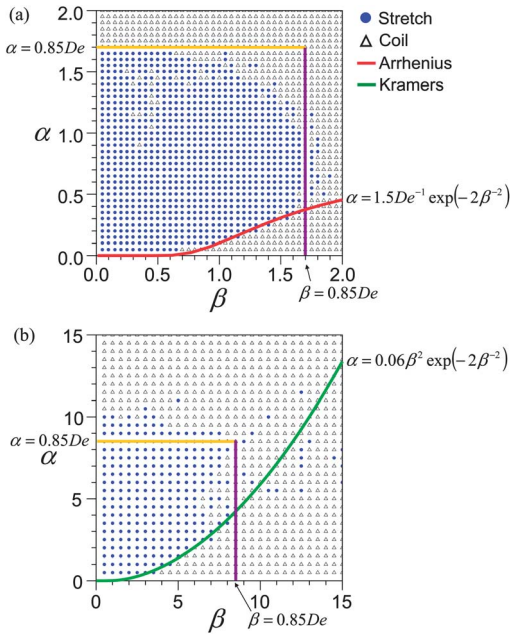

Fig. 13 Calculated coil–stretch phase diagrams for (a) $De = 2$ and (b) $De = 10$ corresponding to $1 < De < De_{crit}$ and $De > De_{crit}$ scenarios, respectively. Results basically resemble those sketched in Fig. 11. In both scenarios, despite different hopping kinetics, their phase diagrams are confined by the same horizontal and vertical phase boundaries $\alpha = 0.85De$ and $\beta = 0.85De$.

while the maximum does not drop significantly, leading to an increase in the time average $\overline{\langle X\rangle}$ (see the inset). Such an increase in $\langle X\rangle$ becomes more evident for $De = 10$, as revealed by Fig. 12b in which the level of $\langle X\rangle$ is found to be increased by increasing α from 0.1 to 5. For both cases, further increasing α will decrease $\langle X\rangle$ due to damping by much more rapid travelling wave strokes. These results confirm our speculation that stretching can indeed be better held by preventing hopping *via* increasing the travelling speed below the damping threshold. The calculated coil–stretch phase diagrams are displayed in Fig. 13. Just like Fig. 11, they are basically portrayed as a tongue-like shape in accordance with the criteria found in the preceding subsections.

IX. Applications of travelling wave stretching to dynamic molecular probing

In this section, we put forth to explore the use of travelling-wave stretching in dynamic molecular probing. Similar to single molecule force spectroscopy, a simple molecular detection can be realized by taking a tethered polymer chain as a flying "kite" for capturing target molecules and then monitoring how the chain responds to changes in its mobility and/or elasticity. In addition to molecular detection, one can also apply the stretching to actively regulate adsorption/desorption of extraneous molecules on a stretched polymer. Below we will give two examples to illustrate how to realise these probing and regulation processes. As our focus here is to show the effects at work, we exclude fluctuations for better illuminating the features of the stretching dynamics. While fluctuations tend to reduce the stretch, we anticipate that the results obtained in this section should not change qualitatively.

A. Dynamic stretching under molecular bombardment

We first demonstrate the use of a stretching polymer chain in capturing and sensing target molecules through their specific binding onto the chain. According to our previous study,[13] if these molecules were charged, they would soon be trapped into an array of ionic clouds moving along with an applied travelling wave field, creating a periodic molecular bombardment onto the chain. Assume that the binding of these target molecules onto the chain happens so fast that its mobility μ and elasticity k undergo abrupt changes upon sweeping by a cloud of target molecules. Hence, both μ and k actually vary with time in a stepwise and accumulative manner according to $(\mu,k) = (\mu_0,k_0) + (\Delta\mu,\Delta k)n$, where the subscript "0" denotes the chain's native state, $\Delta\mu$ and Δk stand for the respective changes in the mobility and elasticity, and $n = [(\tau - \tau_1)/T_\omega]$ is the number of target-molecule clouds passing through the chain after an injection of these molecules at time τ_1. Note here that $\Delta\mu$ can be either >0 or <0 due to adsorption of like or unlike charges, whilst Δk is always >0 since the chain would be getting stiffer and stiffer due to the buildup of extraneous molecules on the chain. If such adsorption persists and fluctuation effects are negligible, then the stretching dynamics can be described by the modified equation:

$$\frac{dX}{d\tau} = -\frac{1}{De}(1 + n\varepsilon_k)X + (1 + n\varepsilon_\mu)\varepsilon(X - \alpha\tau), \qquad (14)$$

with $\varepsilon_k = \Delta k/k_0$ and $\varepsilon_\mu = \Delta\mu/\mu_0$ measuring the sizes of the two step changes relative to the values at the native state.

We first look at effects of ε_μ by letting $\varepsilon_k = 0$. Several stretching dynamics are displayed in Fig. 14. For $\varepsilon_\mu > 0$, because of the progressive increase in the electric force, the chain can keep gaining an extension of $\sim\varepsilon_\mu De$ every cycle, and the larger the α the faster the growth (Fig. 14a). Even if the chain starts with a little stretch with large α or small De, the increasing electric force will eventually outweigh the elastic force, making the extension grow with time (see Fig. 14b and c). On the other hand, diminishing the chain's mobility with $\varepsilon_\mu < 0$ will lead the stretch to fall off for the first few cycles until the isoelectric point (*i.e.* $\mu = 0$) at $n \approx 1/\varepsilon_\mu$, as seen in Fig. 14d. If the chain is allowed to be

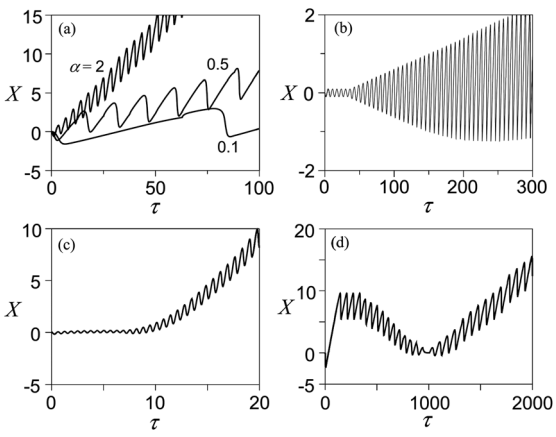

Fig. 14 Various stretching dynamics when subjected to consecutive step changes in the chain's mobility while keeping the chain's elasticity unchanged ($\varepsilon_k = 0$). (a) $\varepsilon_\mu = 0.5$, $De = 2$. (b) $\varepsilon_\mu = 0.5$, $De = 0.1$, $\alpha = 1$. (c) $\varepsilon_\mu = 0.5$, $De = 2$, $\alpha = 10$. (d) $\varepsilon_\mu = -0.1$, $De = 10$, $\alpha = 0.1$.

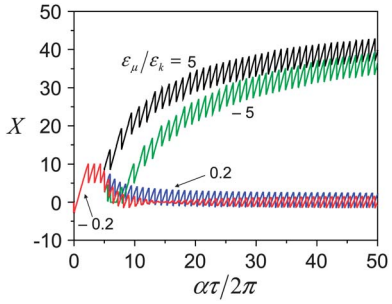

Fig. 15 Stretching responses when subjected to consecutive step changes in both the chain's mobility and elasticity. The stretch is amplified when $|\varepsilon_\mu/\varepsilon_k| > 1$, whereas it is suppressed when $|\varepsilon_\mu/\varepsilon_k| < 1$. $De = 0.1$. $\alpha = 0.01$.

overcharged by absorbing more countercharged molecules beyond the isoelectric point, it can be re-stretched and extended indefinitely by the outgrowing electric force due to the continual buildup of the molecules. In this case, the result will be similar to Fig. 14b or c. As for the case where the chain is only subject to a constant increase in its elasticity, it is clear that it will lose the ability to stretch and hence shrink with time due to the gradually increasing elastic restoring force (not shown).

When both ε_μ and ε_k are present, since the former tends to increase the stretching (at the steady oscillation state) but the latter tends to ease it off, how their combined effects determine the behavior of the stretching would depend on the ratio $\varepsilon_\mu/\varepsilon_k$. As shown in Fig. 15, if $|\varepsilon_\mu|/\varepsilon_k > 1$, the chain's final extent will grow larger than its initial value because the stretch can be amplified more by raising the electric force against elastic retraction (despite the fact that $\varepsilon_\mu/\varepsilon_k < -1$ will decrease the stretch in the beginning). In contrast, $|\varepsilon_\mu|/\varepsilon_k < 1$ will decrease the stretch due to the stronger elastic retraction setup by the greater increment in the elastic force. We also observe (not shown) that changing α only changes the time required to reach a steady oscillation state, but it does not affect the magnitude of the chain's final extent. A close inspection of eqn (14) reveals that the final extent of stretching is controlled by the effective Deborah number, the ratio of the electric force to the elastic force in the $n \to \infty$ limit:

$$De_{\text{eff}} = \frac{|\varepsilon_\mu|}{\varepsilon_k} De. \qquad (15)$$

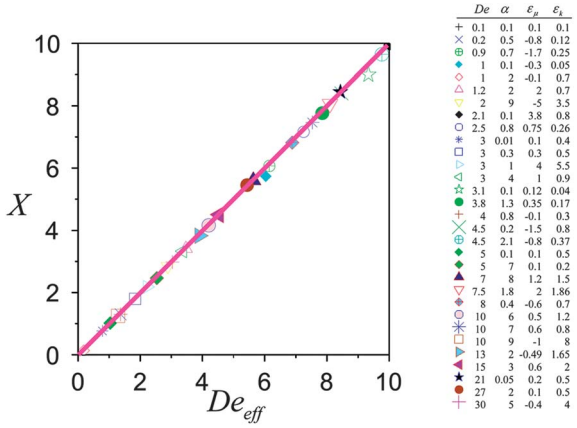

Fig. 16 Long-term maximum chain extensions (symbols) found under various molecular bombardment conditions. All of the data can be collapsed into a single master curve: $X = De_{\text{eff}}$ (line) with $De_{\text{eff}} = De|\varepsilon_\mu/\varepsilon_k|$.

Tracking how the final chain extensions change under various conditions in Fig. 16, we find that they all collapse according to

$$X \approx De_{\text{eff}}. \tag{16}$$

As a result, the stretching with $De < 1$ (>1) will eventually be enlarged (suppressed) with $De_{\text{eff}} > 1$ (<1) if the mobility change is greater (less) than the elasticity increment. Since $X \approx De$ or De/α at the native state (see Section V), the chain's extent is actually changed by a factor of $|\varepsilon_\mu|/\varepsilon_k$ or $\alpha|\varepsilon_\mu|/\varepsilon_k$ in this molecular bombardment process.

B. Use of cyclic stretching in regulating molecular adsorption and desorption

In the second example, we would like to demonstrate that cyclic stretching of a polymer chain can also be used to regulate the adsorptive transport of extraneous solute molecules on the chain. The following assumptions are made to demonstrate this idea. First, we assume that these molecules are irresponsive to electric fields and uniformly distributed over the chain upon adsorption. Second, their transport is assumed not to change the chain's properties and therefore the stretching dynamics. Third, the sorption process here is assumed to be governed by the Langmuir kinetic model.[28] In this model, the adsorptive and desorptive fluxes are prescribed by $k_a C_0(\Gamma_\infty - \Gamma)$ and $-k_d\Gamma$, respectively,

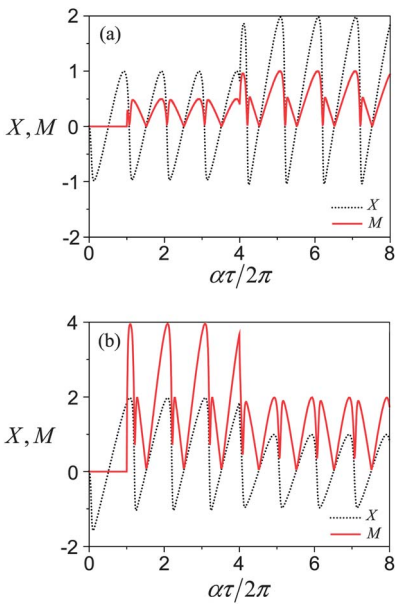

Fig. 17 Use of a cyclically stretching polymer chain in regulating molecular adsorption/desorption over the chain. For slow stretching with $\alpha = 0.1$, a maximum for the absorbed amount M occurs at the corresponding maximum for the chain extension X at the moment when both adsorption and desorption reach an equilibrium. Since the ratio between these two maxima $M_{\max}/X_{\max}$ is equal to the ratio of the adsorption to desorption rates K_1/K_2, this can be used to control adsorption/desorption by changing De. (a) With $(K_1,K_2) = (1,2)$ under which desorption dominates adsorption, adsorption enhancement can be achieved by increasing M *via* increasing De from 1 to 2. (b) With $(K_1,K_2) = (2,1)$, on the other hand, prevailing adsorption can be suppressed by reducing M *via* decreasing De from 2 to 1. In both cases, the changes of De are introduced at the end of the 4th cycle.

where k_a and k_d are the rate constants, Γ is the solute concentration *per surface area* along the chain, Γ_∞ is the maximum packing density, and C_0 is the solute concentration in the bulk. As the chain also works like an extendable cable that can capture/release more solute molecules as it stretches/contracts, this relative motion produces an additional convective flux $\vartheta C_0(\mathrm{d}x/\mathrm{d}t)$ into/out of the chain for adsorption/desorption, where ϑ measures the projection to the chain on the solution side due to the inclination of the chain. Based on the above assumptions, taking mass balance for solute molecules by adding up all the fluxes over the chain surface $\pi|x|d$ (with d being the diameter of the chain), we derive the following equation for determining how the total mass of the solute molecules absorbed on the chain, $\pi d|x|\Gamma$, varies with time:

$$\frac{\mathrm{d}(|x|\Gamma)}{\mathrm{d}t} = \left[k_a C_0(\Gamma_\infty - \Gamma) - k_d\Gamma + \vartheta C_0\frac{\mathrm{d}x}{\mathrm{d}t}\right]|x|.$$

Let $\sigma = \Gamma/(\vartheta b^{-1}C_0)$ be the dimensionless surface concentration. Then the above equation is reduced to the dimensionless form:

$$\frac{\mathrm{d}(|X|\sigma)}{\mathrm{d}\tau} = \left(K_1 - K_2\sigma + \frac{\mathrm{d}X}{\mathrm{d}\tau}\right)|X|, \tag{17}$$

wherein $K_1 = (k_a\Gamma_\infty)/(\vartheta U_0)$ and $K_2 = b^{-1}(k_aC_0 + k_d)/U_0$ measure the importance of adsorption and desorption relative to convection induced by the stretching, respectively, and their ratio provides the sorption constant when adsorption equilibrates with desorption.

In Fig. 17, we observe that as long as the stretching is sufficiently slow ($\alpha < 1$), a maximum for the absorbed amount $M \equiv |X|\sigma$ occurs at the corresponding maximum for X at the moment when both adsorption and desorption reach an equilibrium. The ratio between these two maxima, $M_{\max}/X_{\max}$, can then be used to determine the sorption constant $K_1/K_2 = \sigma_{\max} = M_{\max}/X_{\max}$. This feature can be further utilized to control the amount of absorbed molecules by changing De. As also illustrated in Fig. 17, the amount of absorbed molecules can be increased by raising De when desorption dominates adsorption ($K_1 < K_2$) (Fig. 17a), whereas prevailing adsorption ($K_1 > K_2$) can be suppressed by decreasing De (Fig. 17b). This result also implies that the stretching could be used to enhance the capture of low-affinity molecules onto a polymer chain while preventing undesired adsorption of high-affinity molecules.

X. Concluding remarks

We have analyzed stretching of a tethered polymer chain under the actions of travelling wave electric fields. The stretching here is driven by low-frequency electrophoresis in a time oscillatory fashion. Both deterministic and stochastic studies are also carried out without and with fluctuations, respectively. In the deterministic study, we show that a polymer chain can be extended by cyclic strokes generated by a travelling wave field and that its extension can be maintained in the wave propagation direction. This is very different from the stretching in purely sinusoidal fields in which a polymer chain merely stretches and contracts back and forth without gaining any net stretch after a cycle. As the stretch can be amplified by raising the field intensity but rapidly damped by increasing the wave speed, these two competing effects, characterized respectively by De and α,

determine the averaged extent of stretching. Therefore, the stretching behavior can be judiciously controlled in terms of the electrode size, the chain's properties, and applied field conditions.

In the stochastic study, we look at whether the chain can maintain its stretch in a travelling wave field in the presence of fluctuations. From a kinetic point of view, this is to examine whether a stretched chain can return to the lower-energy coil state through hopping activated by random noises. The situation here can be thought of as a vibrating harmonic oscillator that can exhibit double or multiple wells, depending on the extent of stretching. We find that, even though increasing the wave speed tends to damp stretching, the effects can help the chain keep extended by preventing it from hopping back to the lower-energy coil state. In other words, the coil-to-stretch transition can be expedited in the sense that a travelling wave field, aside from driving the stretching, provides an additional trapping for locking the chain into a stretched state at a higher energy level. In this regard, we identify two distinct hopping kinetics: Arrhenius and Kramers modes, governing the respective coil–stretch transitions in the double-well and multiple-well scenarios. If fluctuations are too large or the wave speed is too high, however, the chain will no longer be stretchable. We develop a kinetic theory to include all these effects and predict tongue-like coil–stretch phase diagrams in good agreement with those generated by Brownian dynamics simulations. It is also worth pointing out that such cooperative effects of AC fields and fluctuations on the dynamic stability of a chain are unique to travelling wave stretching—they simply do not exist in steady or usual AC fields.

We also put forth to explore the possibility of applying travelling wave stretching to dynamic molecular probing. Such probing is illustrated by monitoring the stretching dynamics under periodic molecular bombardments. The stretching can also be applied to regulate molecular adsorption/desorption onto the chain. These examples might open up new paradigms of single molecule spectroscopy for *in situ* molecular probing and detection.

It would be interesting to look at how a polymer chain is folded or unfolded and how its conformation evolves under the influence of travelling wave fields. These issues could be better addressed by modeling a polymer as a bead-spring chain and by resorting to Brownian dynamics simulations again to visualize how it deforms at finer scales. It is anticipated that fluctuation effects would play critical roles in the dynamics at the subchain level. Additional insights may be gained by solving for the configurational probability distribution from the time-dependent Smoluchowski equation. As the present study has revealed some essences about how a polymer chain responds to travelling wave fields with and without fluctuations, it should provide useful prior knowledge for these more sophisticated studies.

Acknowledgements

This work was supported by the National Science Council of Taiwan under Grants 97-2628-E-006-001-MY3 and 100-2221-E-006-185 of HHW.

References

1 A. Bensimon, A. Simon, A. Chiffaudel, V. Croquette, F. Heslot and D. Bensimon, *Science*, 1994, **265**, 2096–2098.
2 E. Y. Chan, N. M. Goncalves, R. A. Haeusler, A. J. Hatch, J. W. Larson, A. M. Maletta, G. R. Yantz, E. D. Carstea, M. Fuchs, G. G. Wong, S. R. Gullans and R. Gilmanshin, *Genome Res.*, 2004, **14**, 1137–1146.
3 J. H. Kim, V. R. Dukkipati, S. W. Pang and R. G. Larson, *Nanoscale Res. Lett.*, 2007, **2**, 185–201.
4 B. Maier, D. Bensimon and V. Croquette, *Proc. Natl. Acad. Sci. U. S. A.*, 2000, **97**, 12002–12007.
5 G. S. Manning, *J. Chem. Phys.*, 1969, **51**, 924–933.
6 F. Oosawa, *Polyelectrolytes*, M. Dekker, New York, 1971.
7 V. A. Bloomfield, *Biopolymers*, 1997, **44**, 269–282.
8 S.-F. Hsieh and H.-H. Wei, *Phys. Rev. E: Stat., Nonlinear, Soft Matter Phys.*, 2009, **79**, 021901.
9 M. D. Wang, H. Yin, R. Landick, J. Gelles and S. M. Block, *Biophys. J.*, 1997, **72**, 1335–1346.
10 S. B. Smith, L. Finzi and C. Bustamante, *Science*, 1992, **258**, 1122–1126.
11 P. S. Doyle, B. Ladoux and J.-L. Viovy, *Phys. Rev. Lett.*, 2000, **84**, 4769–4772.
12 S. Ferree and H. W. Blanch, *Biophys. J.*, 2003, **85**, 2539–2546.
13 H.-H. Wei, *Appl. Phys. Lett.*, 2007, **90**, 204103.
14 P. G. De Gennes, *J. Chem. Phys.*, 1974, **60**, 5030–5042.
15 V. Namasivayam, R. G. Larson, D. T. Burke and M. A. Burns, *Anal. Chem.*, 2002, **74**, 3378–3385.
16 P. T. Underhill and P. S. Doyle, *Phys. Rev. E: Stat., Nonlinear, Soft Matter Phys.*, 2007, **76**, 011805.
17 S.-F. Hsieh, C.-P. Chang, Y.-J. Juang and H.-H. Wei, *Appl. Phys. Lett.*, 2008, **93**, 084103.
18 A. C. Hindmarsh, *ACM SIGNUM Newsletter*, 1980, **15**, 10–11.
19 M. Ueda, K. Yoshikawa and M. Doi, *Polym. J.*, 1997, **29**, 1040–1043.
20 M. Ueda, K. Yoshikawa and M. Doi, *Polym. J.*, 1999, **31**, 637–644.
21 S. Wang, H. C. Chang and Y. Zhu, *Macromolecules*, 2010, **43**, 7402–7405.
22 H. Liu, Y. Zhu and E. Maginn, *Macromolecules*, 2010, **43**, 4805–4813.
23 P.-Y. Hsiao, Y.-F. Wei and H.-C. Chang, *Soft Matter*, 2011, **7**, 1207–1213.
24 H. P. Babcock, R. E. Teixeira, J. S. Hur, E. S. G. Shaqfeh and S. Chu, *Macromolecules*, 2003, **36**, 4544–4548.
25 V. A. Beck and E. S. G. Shaqfeh, *J. Chem. Phys.*, 2006, **124**, 094902.
26 H. A. Kramers, *Physica*, 1940, **7**, 284–304.
27 W. C. K. Poon and D. Andelman, *Soft Condensed Matter Physics in Molecular and Cell Biology*, Taylor & Francis, New York, 2006.
28 J. C. Berg, *An Introduction to Interfaces & Colloids: the Bridge to Nanoscience*, World Scientific, Singapore, 2010.

